

Polarization-independent Optical Broadband Angular Selectivity

Yurui Qu,^{†,‡} Yichen Shen,^{*,†} Kezhen Yin,[§] Yuanqing Yang,[#] Qiang Li,[‡] Min Qiu,[‡] and Marin

Soljačić[†]

[†]Department of Physics, Massachusetts Institute of Technology, Cambridge, Massachusetts 02139, USA

^{*}State Key Laboratory of Modern Optical Instrumentation, College of Optical Science and Engineering, Zhejiang University, Hangzhou 310027, China

[§]Mantoline Corporation, Mantua, OH 44255, USA

[#]Centre for Nano Optics, University of Southern Denmark, Campusvej 55, DK-5230, Denmark

KEYWORDS: angular selectivity, polarization-independent, photonic crystals, birefringence

ABSTRACT: Generalizing broadband angular selectivity to both polarizations has been a scientific challenge for a long time. Previous demonstrations of the broadband angular selectivity work only for one polarization. In this paper, we propose a method that can achieve polarization-independent optical broadband angular selectivity. Our design is based on a material system consisting of alternating one-dimensionally anisotropic photonic crystal (1D PhC) stacks and half wave plates. 1D PhC stacks have an angular photonic band gap for p-polarized light and half wave plates can convert s-polarized light to p-polarized light. By introducing alternating 1D PhC stacks and half wave plates, we predict that one can achieve a central transmission angle at normal incidence and an angularly selective range of less than 30° across the whole visible spectrum.

The frequency, the polarization, and the propagation direction are three fundamental properties of a monochromatic plane wave (apart from its phase and amplitude). The ability to select light based on these three separate properties is of paramount importance for tailoring the flow of light. Among these three, selecting light according to the propagation direction, which is known as angular selectivity, has long been a scientific challenge and could be of a significant benefit for a number of applications, including high-efficiency solar energy conversion,¹⁻³ privacy protection,^{4, 5} and detectors with enhanced signal-to-noise ratios.⁶ Methods based on metamaterials^{7, 8} and photonic crystals^{9, 10} have been explored for angular selectivity; however, they can only offer narrowband angular selectivity because of the inherent resonant properties. Ideally, an angularly selective system should work over a broadband spectrum.

Several strategies to achieve broadband angular selectivity have also been investigated. (i) For example, the micro-louvre approach was proposed by 3M, Inc,⁴ while parabolic directors were investigated by Atwater and co-workers.¹¹ The components of the micro-louvre or the parabolic directors are much bigger than the wavelength of the visible light, so laws of geometrical optics still hold. Besides, successful experimental demonstrations of the parabolic directors have so far been limited to small scale due to the difficulties in high-resolution large scale fabrication. (ii) A variety of methods that work for only one of the polarizations have also been investigated. These include: methods based on combination of polarizers and birefringent films,¹² anisotropic metamaterials,¹³ Brewster modes in metamaterials,¹⁴ and metallic gratings.¹⁵ The fact that these work only for one polarization (Figure 1 (a) and (b)) greatly limits some of their applications such as high-efficiency solar energy harvesting and car window shield. For solar energy conversion, a recent theoretical work from Atwater's group has predicted that by limiting the light emission angle, it is possible to significantly increase absolute efficiency for GaAs solar cells with ideal back reflector.² Compared

with the existing angular selectivity technologies working for only one polarization, the polarization-insensitive technology performs better in solar energy conversion because sunlight is randomly polarized. Another promising application is for car window shield. As we know, strong direct sunlight is very dangerous for drivers to have traffic accidents. Angular selectivity film on car window shield can keep drivers' viewing angle transparent as usual (transparent at viewing angles), but block the direct sunlight (reflective at other angles). In this case, the angular selectivity technology has to be polarization-insensitive because of randomly polarized sunlight.

In 2014, Shen et al. proposed that one can utilize the Brewster angle of two isotropic dielectric media to achieve single-polarization broadband angular selectivity.¹⁶ They also proposed that angular selectivity could be achieved for both polarizations using materials with permeability $\mu \neq 1$. However, it is very difficult to achieve this in the visible range because most materials have permeability $\mu \approx 1$. Moreover, even if one cares only about a single polarization, the Brewster angle of two dielectric media is always larger than 45° (in the lower index material). In many applications such as privacy protection screens, having a central transmission angle at normal incidence and a selective angle smaller than 30° (viewing angle from -30° to 30°) are highly desirable. There has yet to emerge a solution to realize a polarization-independent broadband angularly selective system without the limitations of geometrical optics and with a central transmission angle at normal incidence and an angularly selective range of less than 30°.

In this paper, we introduce a method that can in principle achieve polarization-independent optical broadband angular selectivity (Figure 1 (c) and (d)). Our design rests on (i) the existence of an angular photonic band gap for p-polarized light within 1D PhC stacks consisting of alternating isotropic and anisotropic layers,¹³ (ii) the fact that a half wave plate (HWP) can convert s-polarized

light to p-polarized light over a limited wavelength range,^{17, 18} and (iii) the fact that alternating 1D PhC stacks and half wave plates of different thicknesses can be used to broaden the working wavelength range. We predict this angularly selective material system could work over the entire visible spectrum for both polarizations using realistic material parameters; it has a central transmission angle that is normal incidence; it could be transparent for all colors at incident angles less than 30° and highly reflecting for larger viewing angles.

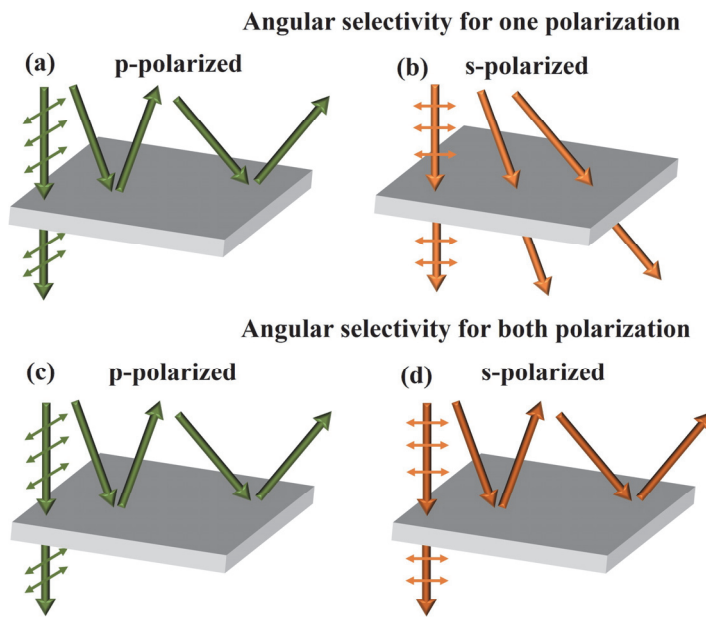


Figure 1. Illustration of angular selectivity on the basis of its polarization. Angular selectivity for single polarization means that (a) p-polarized light is transmitted in one direction and is reflected in all other directions while (b) s-polarized light experiences no angular selectivity. Angular selectivity for both polarizations indicate that both (c) p-polarized and (d) s-polarized light experience angular selectivity over the incident light. So far, achieving angular selectivity for both polarizations has remained elusive.

MATERIALS AND METHODS

We begin with a one-dimensional photonic crystal (1D PhC) consisting of anisotropic layers (A) with permittivity $\epsilon_A = (\epsilon_{xx}^A, \epsilon_{yy}^A, \epsilon_{zz}^A) = (2.56, 2.56, 2.25)$ and isotropic layers (B) with permittivity $\epsilon_B = 2.56$. As mentioned above, the selective angle of 1D PhC consisting of only isotropic materials is limited by the Brewster angle and is always larger than 45° . However, we can achieve normal angle transparency using the 1D PhC consisting of anisotropic and isotropic layers. To understand how this material system can achieve normal angle transparency, we look at the analytical expressions for the effective refractive index n_A of the anisotropic layer (A) for both s-polarized and p-polarized light as follows¹³:

$$n_A^s = \frac{1}{\sqrt{\frac{\cos^2 \theta_A^s}{\mu_{xx}^A \epsilon_{yy}^A / \mu_0 \epsilon_0} + \frac{\sin^2 \theta_A^s}{\mu_{zz}^A \epsilon_{yy}^A / \mu_0 \epsilon_0}}} , \quad (1)$$

$$n_A^p = \frac{1}{\sqrt{\frac{\cos^2 \theta_A^p}{\mu_{yy}^A \epsilon_{xx}^A / \mu_0 \epsilon_0} + \frac{\sin^2 \theta_A^p}{\mu_{yy}^A \epsilon_{zz}^A / \mu_0 \epsilon_0}}} , \quad (2)$$

where θ_A^s and θ_A^p are the refraction angles for s-polarized and p-polarized light in layer A, as described by Snell's law:

$$n_A^s \sin \theta_A^s = n_{air} \sin \theta_{inc}, \quad (3)$$

$$n_A^p \sin \theta_A^p = n_{air} \sin \theta_{inc}. \quad (4)$$

From equations (1) and (2), considering $\mu=1$ for most real materials, we can see that s-polarized light is only affected by ϵ_{yy}^A , while p-polarized light is affected by ϵ_{xx}^A and ϵ_{zz}^A . In particular, p-polarized light is affected by ϵ_{zz}^A when incident angle is away from the normal, while s-polarized light is not. At normal incidence, both s-polarized light and p-polarized light are not affected by ϵ_{zz}^A and "see" the same refractive index of material A and B ($\sqrt{\epsilon_{xx}^A} = \sqrt{\epsilon_{yy}^A} = \sqrt{\epsilon_B}$), so both s-polarized and p-polarized light are transmitted. At nonzero angles, incident s-polarized light still "sees" the same refractive indexes for material A and B because s-polarized light is not affected by ϵ_{zz}^A . However, p-polarized light incident at nonzero angle "sees" different refractive indexes for material A and B because p-polarized light is affected by ϵ_{zz}^A , as shown in eq

2. We know that if a 1D photonic crystal has two materials A and B with different refractive indexes, there will be a photonic bandgap.¹⁹ Therefore, a stack of 1D PhCs opens an angular band gap only for p-polarized light; p-polarized light experiences total transmission at normal incidence while experiencing total reflections at large oblique incident angles. Note the permittivity $\epsilon_A = (2.56, 2.56, 2.25)$ is chosen because this material can be easily achieved using widely used polymers^{20, 21} and mature mechanical methods in industry²²⁻²⁵. Higher anisotropy in permittivity ϵ would result in higher index contrast and wider frequency gaps for incidence angles not close to the normal. To cover the entire visible spectrum, 1D PhC layers with various periodicities could be stacked together to enlarge the band gap (see Figure 2 (a)). We consider a multilayer structure consisting of 80 such stacks, each stack consisting of 100 isotropic-anisotropic bilayers. In our material system, 80 stacks is the minimum number of stacks we need to cover the entire visible spectrum. The period of the i th stack ($i = 1, 2, \dots, 80$) should be $1.01^{(i-1)}a_1$, where a_1 is the period of the first stack facing the incident light ($a_1=130$ nm). 100 isotropic-anisotropic bilayers are required for an angularly selective range of less than 30°. Narrower angular range can be achieved by increasing the number of bilayers. The simulation results indicate that such 1D PhC stacks provide angular selectivity for p-polarized light and are nearly transparent for s-polarized light over the entire visible spectrum (Figure 2 (b) and (c)). The simulation is based on the rigorous coupled wave analysis (RCWA).²⁶

Several methods have been studied to achieve polarization-insensitive spatial light modulation, such as half-wave plate,²⁷ nematic liquid-crystal (LC) combined with mirror,²⁸ blue-phase liquid crystal over silicon device,²⁹ and two orthogonal LC layers are separated by two ultra-thin anisotropic polymer films³⁰. The ideas can be borrowed and help to achieve polarization-insensitive angular selectivity. In this manuscript, we choose half-wave plate because it is easy to be integrated into multi-layer film system. Based on the discussions above, we propose a material system to achieve polarization-independent angular selectivity (Figure 2 (d)). The material system consists of alternating 1D PhC stacks and half wave plates. The half wave plate is a

birefringent film with permittivity $\epsilon = (2.56, 2.25, 2.56)$. The permittivity is chosen according to the available polymers in industry^{20, 21}. All 1D PhC stacks in Figure 2 (d) are the same with 80 stacks, each stack consisting of 100 bilayers. p-polarized light is reflected by 1D PhC at large incident angle and is transmitted at small incident angle, and therefore angular selectivity is realized. s-polarized light is totally transmitted in the 1D PhC, and is subsequently transformed into p-polarized light after passing through a half wave plate. The “new” p-polarized light will then be reflected by the following 1D PhC[†], so both s-polarized and p-polarized light experience angular selectivity. However, each half wave plate can work only for a limited wavelength range. By cascading half wave plates of different thicknesses, broadband angular selectivity can be realized. A large range of polymers can be selected as the materials of 1D PhCs and half wave plate, such as polyethylene terephthalate (PET), polycarbonate (PC), polystyrene (PS), and polyurethane (PU). All polymers above are optical grade polymers and exhibit glass-like transparency with negligible losses. They have similar refractive index to what we use in our simulations. Anisotropic refractive indexes of these polymers can be achieved based on mature mechanical methods such as compression²², shear stress²³, uniaxial/biaxial orientation²⁴, and electric field²⁵.

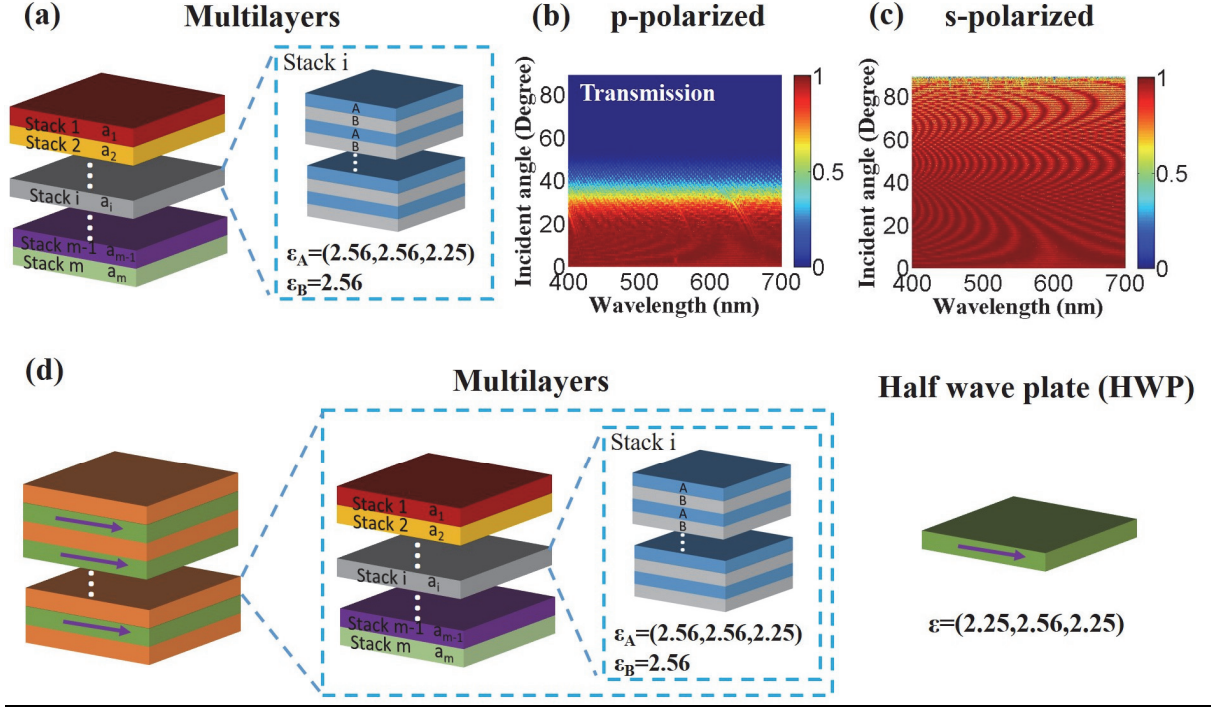


Figure 2. (a) Schematic of one-dimensional photonic crystal (1D PhC) consisting of 80 stacks, each stack consisting of 100 isotropic-anisotropic bilayers. A is an anisotropic material with permittivity $\epsilon_A = (2.56, 2.56, 2.25)$; B is an isotropic medium with permittivity $\epsilon_B=2.56$. (b) p-polarized and (c) s-polarized transmission spectrum for 1D PhC consisting of 80 stacks, each stack consisting of 100 isotropic-anisotropic bilayers. 1D PhC stacks provide broadband angular selectivity only for p-polarized light, not for s-polarized light. (d) Schematic of our design that can provide polarization-independent broadband angular selectivity. The material system consists of alternating 1D PhC stacks and half wave plates. The half wave plate that can convert s-polarized light to p-polarized light is a birefringent film with permittivity $\epsilon= (2.25, 2.56, 2.25)$. The birefringent axis which is in the direction of $\epsilon_{xx}^{HWP}=2.25$ is marked by purple arrow.

RESULTS AND DISCUSSION

A half wave plate can convert s-polarized light to p-polarized light within a certain limited wavelength range. The ratio of p-polarized light is defined by the portion of the p-polarized transmission energy flux in the total transmission energy flux ($I_{p, \text{trans}}/I_{\text{total, trans}}$) when the incident light is s-polarized. We study the ratio of

transmitted p-polarized light from an s-polarized incident beam at different wavelengths for a half wave plate with permittivity $\epsilon = (2.25, 2.56, 2.25)$. The light is incident from air in all simulations in this paper. The incident plane is at the angle of 45° with respect to the birefringent axis. At the central wavelength (λ_1), s-polarized light can be completely converted to p-polarized light using one half wave plate (Figure 3 (b)). The relation of the thickness to the central wavelength of one wave plate is given by $\delta = (2\pi\Delta n \times L)/\lambda_1$, where δ is the retardation of the phase, which equals π for half wave plate; Δn is the refractive index difference of the birefringent film, which is 0.1 for our calculation; L is the thickness of the wave plate; λ_1 is the central wavelength of the wave plate. We set $L = 2.75 \mu\text{m}$, so the central wavelength λ_1 is 550 nm.

When the incident light shifts away from the central wavelength, the ratio of the p-polarized light decreases. Part of the s-polarized light still maintains its polarization after passing through the half wavelength plate, which decreases the efficiency of the angular selectivity of s-polarized light. To achieve better performance of broadband angular selectivity, we cascade half wave plates with different thicknesses. The ratio of p-polarized light for half wave plates with different thicknesses is calculated (Figure 3 (a)). The central wavelength of the half wave plate increases as the thickness is increased. The central wavelengths of half wave plates with thicknesses ranging from $1.925 \mu\text{m}$ to $3.575 \mu\text{m}$ cover the entire visible spectrum. In addition, it turns out that the ratio of p-polarized light is not very sensitive to the incident angle (Figure 3 (b)). When the incident angle increases, the central wavelength and the efficiency remain almost constant. The ripples of the ratio of p-polarized light result from the effect of Fabry–Pérot cavity caused by the half wave plate itself.

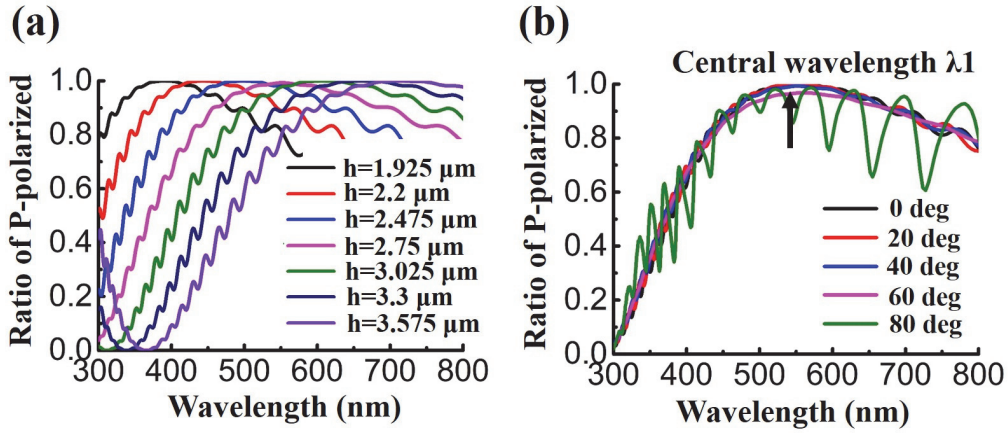


Figure 3. (a) Ratio of p-polarized light versus wavelength for half wave plates with different thicknesses at normal incidence. All or part of s-polarized light can transform into p-polarized light after it passes through the half wave plate. (b) Ratio of p-polarized light versus wavelength at different incident angle. At the central wavelength λ_1 of one half wave plate, s-polarized light can totally transform into p-polarized light. The thickness of the half wave plate is fixed at $L = 2.75 \mu\text{m}$.

To show the performance of angular selectivity in the visible spectrum, we explore three composite-structures with different number (1, 5 and 13) of half wave plates. Each of the composite-structures consists of the structures shown in Figure 2 (d). The incident plane i is at the angle of 45° with respect to the birefringent axis (Figure 4(a)). All three structures show a good performance of angular selectivity for p-polarized light because 1D PhC stacks themselves provide angular selectivity for only p-polarized light (Figure 4 (b), (d) and (f)). The first structure contains a single half wave plate whose thickness is $2.75 \mu\text{m}$. Such structure shows low transmission at the central wavelength around 550 nm, because s-polarized light transforms into p-polarized light after passing through the half wave plate and is reflected by the following 1D PhC (Figure 4 (c)). However, when the wavelength is shifted substantially away from the central wavelength, the transmission increases because a part of s-polarized light still maintains its polarization after passing through the half wave plate and is hence transmitted through the entire structure.

Compared to only a single half wave plate, the structure with 5 half wave plates presents better

performance for s-polarized light (Figure 4 (e)). Thicknesses of the 5 layers are chosen at regular intervals away from $L = 2.75 \mu\text{m}$: $2.063 \mu\text{m}$ ($0.75L$), $2.406 \mu\text{m}$ ($0.875L$), $2.75 \mu\text{m}$ (L), $3.094 \mu\text{m}$ ($1.125L$), and $3.438 \mu\text{m}$ ($1.25L$). The central wavelengths of 5 half wave plates with thicknesses chosen in such manner are at regular intervals and cover nearly the entire visible spectrum. Thus s-polarized light can be transformed into p-polarized light in the entire visible spectrum and be reflected by the 1D PhC to remove most of the transmission modes. Even more half wave plates can be added to get better performance (Figure 4 (g)). Thicknesses of the 13 layers increase from $1.925 \mu\text{m}$ to $3.575 \mu\text{m}$ with a 137.5 nm step, so the thicknesses equal $0.7L$, $0.75L$, $0.8L$, ..., $1.25L$, $1.3L$, respectively. The central wavelengths of these 13 half wave plates again cover the whole visible spectrum at regular intervals. This structure achieves an angularly selective range of less than 30° for both polarizations over the entire visible spectrum (Figure 4 (f) and (g)).

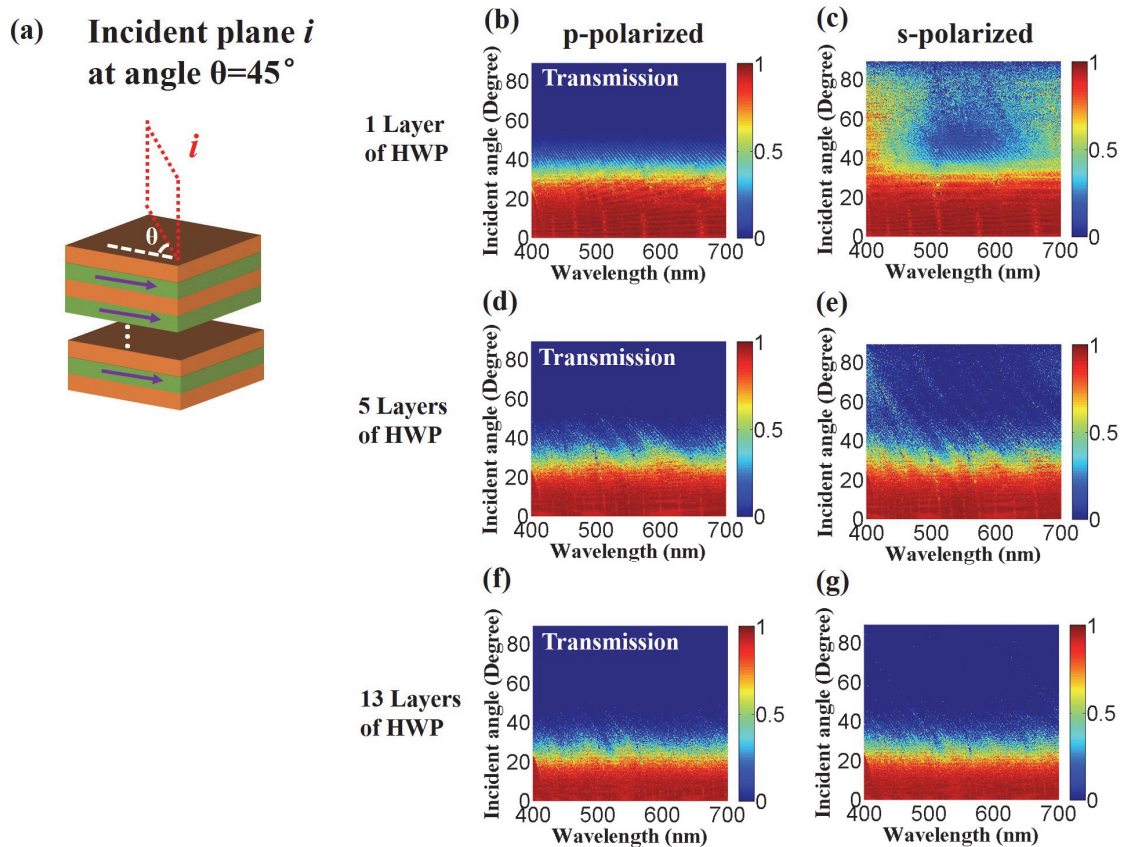


Figure 4. (a) Schematic of our design that can provide polarization-independent broadband angular selectivity. The

transmission spectrum is calculated when the incident plane is at the angle of 45° with respect to the birefringent axis. (b) p-polarized and (c) s-polarized transmission spectrum for a structure containing one half wave plate. (d) p-polarized and (e) s-polarized transmission spectrum for a structure containing 5 layers of half wave plates. (f) p-polarized and (g) s-polarized transmission spectrum for a structure containing 13 layers of half wave plates.

The design in Figure 4 (a) can provide broadband angular selectivity for p-polarized light at different incident planes because all p-polarized light at larger incident angles can be reflected on the top 1D PhC stacks (see Figure S1 in Supporting Information). However, it can only provide perfect angular selectivity at one incident plane for s-polarized light. This incident plane is located at the angle of 45° with respect to the birefringent axis where the s-polarized light at central wavelength can be completely converted into p-polarized light (Figure 3). When the incident plane rotates away from the 45° incident plane, more s-polarized light can transmit the whole structure at large incident angle because less s-polarized light can be converted into p-polarized light (see Figure S2). In a special case, the s-polarized light can totally transmit when the incident plane contains the birefringent axis ($\theta=0^\circ$). The s-polarized light “sees” a uniform material when the polarization is in the direction of the birefringent axis.

To achieve broadband angular selectivity for all incident planes, we design a structure with rotating birefringent axes of the half wave plates (Figure 5(a)). The structure contains 20 layers of the half wave plates which are divided to 5 groups. The thicknesses of 5 groups are chosen as: $2.063 \mu\text{m}$ ($0.75L$), $2.406 \mu\text{m}$ ($0.875L$), $2.75 \mu\text{m}$ (L), $3.094 \mu\text{m}$ ($1.125L$), and $3.438 \mu\text{m}$ ($1.25L$), respectively. Each group consists of 4 layers of half wave plates with the same thickness. The birefringent axis of each half wave plate rotates 22.5° with respect to the top one, as shown in Figure 5(b). The rotating half wave plates enlarge the angular range of incident planes at which s-polarized light can be converted to p-polarized light. After we test different layers of rotating half wave plates, 4 layers is the least number of half wave plates that can achieve angular selectivity at all

incident planes. As shown in Figure 5(c), the structure shows a good performance of angular selectivity for incident planes ranging from 0° to 80° with the step of 10° .

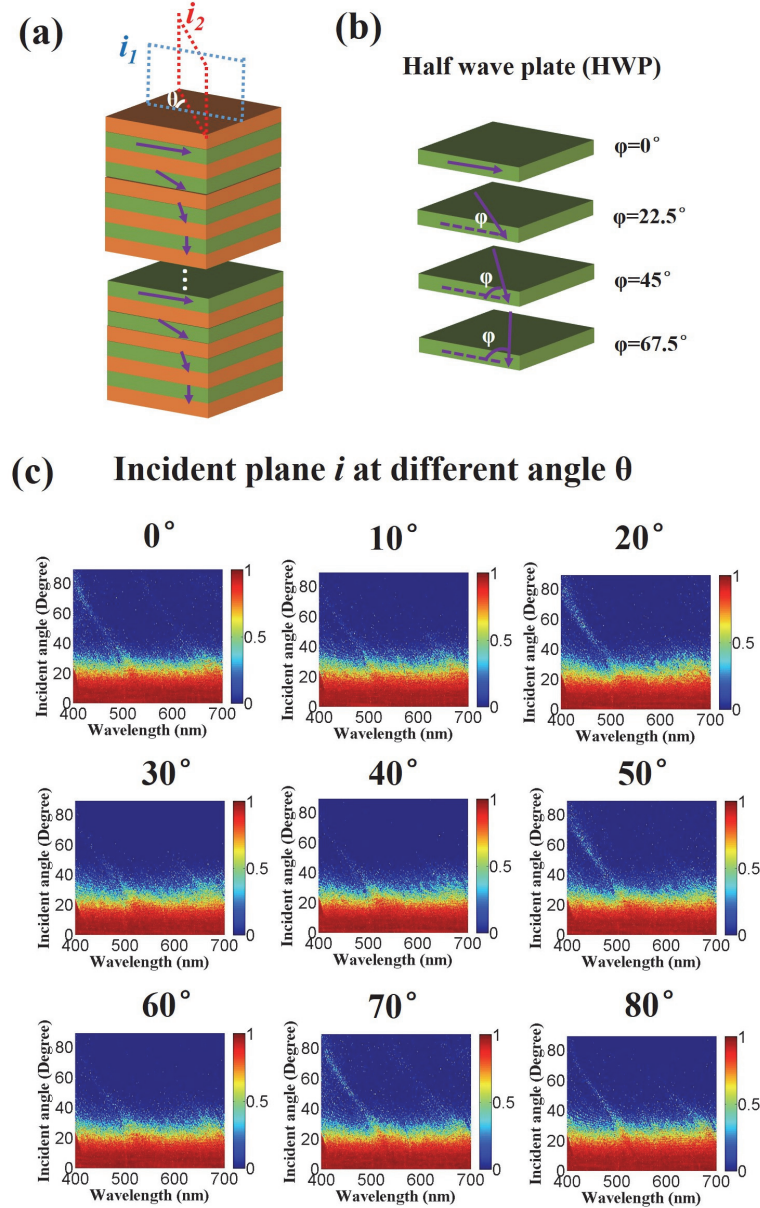


Figure 5. (a) Schematic of our design that can provide polarization-independent broadband angular selectivity for all incident planes. The material system consists of alternating 1D PhC stacks and half wave plates. The total 20 layers of the half wave plates are divided to 5 groups whose thicknesses are chosen as $0.75L, 0.875L, 2.75L, 1.125L$, and $1.25L$ ($L = 2.75 \mu\text{m}$). (b) In each group, the birefringent axis of the half wave plate with the same thickness rotates at regular intervals: $0^\circ, 22.5^\circ, 45^\circ$, and 67.5° . (c) s-polarized transmission spectrum for a structure containing 20 layers of half wave plates at different incident planes

In conclusion, we present a method that can achieve polarization-independent optical broadband angular selectivity. The key idea in our design is to use a material system consisting of alternating 1D anisotropic PhC stacks and half wave plates. We achieve an angularly selective range of less than 30° for both polarizations over the entire visible spectrum. All the materials in our simulation are selected according to the widely used polymers and mature mechanical manufacturing methods in the industry. The material system with loss is also discussed in the Fig. S4 in Supporting Information. The transmission can still be higher than 80% by optimizing the number of stacks and the periods of bilayers. Such material systems could be used in many applications such as high-efficiency solar energy conversion, privacy protection, and detectors with enhanced signal-to-noise ratios.

FOOTNOTE

† Note that as it travels backwards through the half wave plate, it gets transformed back into s-polarization, and can hence exit the structure freely.

AUTHOR INFORMATION

Corresponding Author

*E-mail: ycshen@mit.edu

Notes

The authors declare no competing financial interest.

ACKNOWLEDGEMENTS

Research supported as part of the Army Research Office through the Institute for Soldier Nanotechnologies under contract no. W911NF-18-2-0048 and W911NF-13-D-0001 (photon management for developing nuclear-TPV and fuel-TPV mm-scale-systems). Also supported as part of the S3TEC, an Energy Frontier Research Center funded by the US Department of Energy under

grant no. DE-SC0001299 (for fundamental photon transport related to solar TPVs and solar-TEs).

This work was also supported by the National Key Research and Development Program of China

(2017YFA0205700) and the National Natural Science Foundation of China (Grant No. 61425023).

Yurui Qu was supported by Chinese Scholarship Council (CSC No. 201706320254). We thank

Duncan Wheeler for comments.

SUPPORTING INFORMATION

The Supporting Information is available free via the Internet at <http://pubs.acs.org>.

REFERENCES

- (1) Kosten, E. D.; Kayes, B. M.; Atwater, H. A. Experimental demonstration of enhanced photon recycling in angle-restricted GaAs solar cells. *Energy Environ. Sci.* **2014**, *7*, 1907-1912.
- (2) Kosten, E. D.; Atwater, J. H.; Parsons, J.; Polman, A.; Atwater, H. A. Highly efficient GaAs solar cells by limiting light emission angle. *Light-Sci. Appl.* **2013**, *2*, e45.
- (3) Höhn, O.; Peters, M.; Ulbrich, C.; Hoffmann, A.; Schwarz, U. T.; Bläsi, B. Optimization of angularly selective photonic filters for concentrator photovoltaic. *Proc. SPIE* **2012**, *8438*, 84380A.
- (4) Clarke, G. M.; Graham, P. D.; Hansen, B. R.; Hoium, T. B.; Slama, D. F. Privacy film. U.S. patent 7,467,873B2, December 23, 2008.
- (5) MacMASTER, S. W. Privacy screen for a display. U.S. patent 7,052,746, May 30, 2006.
- (6) Shen, Y.; Hsu, C. W.; Yeng, Y. X.; Joannopoulos, J. D.; Soljačić, M. Broadband angular selectivity of light at the nanoscale: Progress, applications, and outlook. *Appl. Phys. Rev.* **2016**, *3*, 11103.
- (7) Schwartz, B. T.; Piestun, R. Total external reflection from metamaterials with ultralow refractive index. *JOSA B* **2003**, *20*, 2448-2453.

- (8) Alekseyev, L. V.; Narimanov, E. E.; Tumkur, T.; Li, H.; Barnakov, Y. A.; Noginov, M. A. Uniaxial epsilon-near-zero metamaterial for angular filtering and polarization control. *Appl. Phys. Lett.* **2010**, *97*, 131107.
- (9) Qian, Q.; Xu, C.; Wang, C. All-dielectric polarization-independent optical angular filter. *Sci. Rep.* **2017**, *7*, 16574.
- (10) Üpping, J.; Miclea, P. T.; Wehrspohn, R. B.; Baumgarten, T.; Greulich-Weber, S. Direction-selective optical transmission of 3D fcc photonic crystals in the microwave regime. *Photonics Nanostruct.* **2010**, *8*, 102-106.
- (11) Atwater, J. H.; Spinelli, P.; Kosten, E.; Parsons, J.; Van Lare, C.; Van de Groep, J.; Garcia De Abajo, J.; Polman, A.; Atwater, H. A. Microphotonic parabolic light directors fabricated by two-photon lithography. *Appl. Phys. Lett.* **2011**, *99*, 151113.
- (12) Winker, B. K.; Taber, D. B. Staggered waveplate LCD privacy screen. U.S. patent 6,239,853, May 29, 2001.
- (13) Hamam, R. E.; Celanovic, I.; Soljačić, M. Angular photonic band gap. *Phys. Rev. A* **2011**, *83*, 35806.
- (14) Shen, Y.; Ye, D.; Wang, L.; Celanovic, I.; Ran, L.; Joannopoulos, J. D.; Soljačić, M. Metamaterial broadband angular selectivity. *Phys. Rev B* **2014**, *90*, 125422.
- (15) Alu, A.; Aguanno, G. D.; Mattiucci, N.; Bloember, M. J. Plasmonic Brewster angle: broadband extraordinary transmission through optical gratings. *Phys. Rev. Lett.* **2011**, *106*, 123902.
- (16) Shen, Y.; Ye, D.; Celanovic, I.; Johnson, S. G.; Joannopoulos, J. D.; Soljačić, M. Optical broadband angular selectivity. *Science* **2014**, *343*, 1499-1501.
- (17) Pancharatnam, S. Achromatic combinations of birefringent plates. Proceedings of the Indian Academy of Sciences-Section A, Springer India, 1955; Vol. 41, No. 4, pp. 130-136.

- (18) Title, A. M. Improvement of Birefringent Filters. 2: Achromatic Waveplate. *Appl. Optics* **1975**, *14*, 229-237.
- (19) Joannopoulos, J. D.; Steven, G. J.; Joshua, N. W.; Robert, D. M. *Photonic crystals: molding the flow of light*; Princeton university press, 2011.
- (20) Nagatoshi, F.; Arakawa, T. Structure of doubly oriented nylon 6. *Polym. J.* **1970**, *1*, 685.
- (21) Cakmak, M.; White, J. L.; Spruiell, J. E. Optical properties of simultaneous biaxially stretched poly (ethylene terephthalate) films. *Polym. Eng. Sci.* **1989**, *29*, 1534-1543.
- (22) Van Aken, J. A.; Janeschitz-Kriegl, H. Simultaneous measurement of transient stress and flow birefringence in one-sided compression (biaxial extension) of a polymer melt. *Rheol. Acta* **1981**, *20*, 419-432.
- (23) Schmidt, G.; Nakatani, A. I.; Butler, P. D.; Karim, A.; Han, C. C. Shear orientation of viscoelastic polymer-clay solutions probed by flow birefringence and SANS. *Macromolecules* **2000**, *33*, 7219-7222.
- (24) Yin, K.; Zhou, Z.; Schuele, D. E.; Wolak, M.; Zhu, L.; Baer, E. Effects of interphase modification and biaxial orientation on dielectric properties of poly (ethylene terephthalate)/poly (vinylidene fluoride-co-hexafluoropropylene) multilayer films. *ACS Appl. Mater. Inter.* **2016**, *8*, 13555-13566.
- (25) Ren, H.; Wu, S. T. Tunable electronic lens using a gradient polymer network liquid crystal. *Appl. Phys. Lett.* **2003**, *82*, 22-24.
- (26) Liu, V.; Fan, S. S4: A free electromagnetic solver for layered periodic structures. *Comput. Phys. Commun.* **2012**, *183*, 2233-2244.
- (27) Liu, J.; Wang, J. Demonstration of polarization-insensitive spatial light modulation using a single polarization-sensitive spatial light modulator. *Sci. Rep.* **2015**, *5*, 9959.

- (28) Love, G. D. Liquid-crystal phase modulator for unpolarized light. *Appl. Optics* **1993**, 32 (13), 2222-2223.
- (29) Hyman, R. M.; Lorenz, A.; Morris, S. M.; Wilkinson, T. D. Polarization-independent phase modulation using a blue-phase liquid crystal over silicon device. *Appl. Optics* **2014**, 53 (29), 6925-6929.
- (30) Lin, Y. H.; Ren, H.; Wu, Y. H.; Zhao, Y.; Fang, J.; Ge, Z.; Wu, S. T. Polarization-independent liquid crystal phase modulator using a thin polymer-separated double-layered structure. *Opt. express* **2005**, 13(22), 8746-8752.